Non-universal finite-size scaling of rough surfaces

2009 J. Phys. A: Math. Theor. 42 485004

(http://iopscience.iop.org/1751-8121/42/48/485004)

IOP PUBLISHING JOURNAL OF PHYSICS A: MATHEMATICAL AND THEORETICAL

J. Phys. A: Math. Theor. **42** (2009) 485004 (15pp) doi:10.1088/1751-8113/42/48/485004

Non-universal finite-size scaling of rough surfaces

Pradipta Kumar Mandal and Debnarayan Jana

Department of Physics, University of Calcutta, 92 A.P.C. Road, Kolkata-700 009, India

E-mail: djphy@caluniv.ac.in

Received 19 June 2009, in final form 9 October 2009
Published 13 November 2009
Online at stacks.iop.org/JPhysA/42/485004

Abstract

We demonstrate the non-universal behavior of finite-size scaling in (1+1) dimension of a nonlinear discrete growth model involving extended particles in a generalized point of view. In particular, we show the violation of the universal nature of the scaling function corresponding to the height fluctuation in (1+1) dimension. The second-order moment of the height fluctuation shows three distinct crossover regions separated by two crossover timescales namely, $t_{\times 1}$ and $t_{\times 2}$. Each regime has different scaling properties. The overall scaling behavior is postulated with a new scaling relation represented as the linear sum of two scaling functions valid for each scaling regime. Besides, we note the dependence of the roughness exponents on the finite size of the system. The roughness exponents corresponding to the rough surface is compared with the growth rate or the velocity of the surface.

PACS numbers: 68.35.Ct, 64.60.al, 61.43.Hv, 05.40.−a

(Some figures in this article are in colour only in the electronic version)

1. Introduction

Theoretical and experimental study of morphology of the growing surfaces and interfaces, which are generated from various different growth processes, is a major challenge in recent years [1–3]. Several discrete models have been proposed to study the morphology of rough surfaces formed in different growth processes such as imbibition in porous media [4–6], thin-film growth in molecular beam epitaxy (MBE) [7, 8] and growth of bacterial colonies [9]. These discrete models are based on simple stochastic growth rules, such as aggregation and diffusion.

The rough surface, evolved from a non-equilibrium process, can be characterized from the study of the moments of the average of height fluctuations, called surface width, defined as

$$W_\gamma(L,t) = \left[\frac{1}{L}\sum_{i=1}^{L}[h(i,t) - \langle h(t)\rangle]^\gamma\right]^{1/\gamma}, \tag{1}$$

where L is the system size, $\langle h(t)\rangle = \frac{1}{L}\sum_{i=1}^{L} h(i,t)$ is the average height over different sites at time t, and γ is the order of the moment of the height fluctuation.

The dynamic formation of the rough surfaces can be realized with the numerical simulation of discrete models. The dynamic and saturated behaviors of the rough surface are characterized with the power-law nature of the moments of height fluctuation. The short time height fluctuation is characterized by exponent β known as dynamic. The saturated behavior of the surface width determines the fractal dimension (represented in terms of the roughness exponent α) of the rough surface. The overall scaling behavior of the rough surface is studied with the Family–Vicsek scaling ansatz [10]. $W_2(L,t)$ is the second-order moment of the height fluctuation; one can write the Family–Vicsek phenomenological scaling ansatz as

$$W_2(L,t) = L^{\alpha} f\left(\frac{t}{L^z}\right), \tag{2}$$

where $z = \alpha/\beta$ and $f(u) \sim u^{\beta}$ $[u \ll 1]$, $f(u) \sim$ constant $[u \gg 1]$. This scaling relation is the central quantity of interest to study the morphology of the surface for any discrete growth process. The values of the exponents α and z uniquely determine the universality classes of the kinetic roughening process. The linear discrete model such as random deposition with surface relaxation (RDSR) [11] and nonlinear discrete models such as the ballistic deposition (BD) model [12], Eden growth (ED) model [13], restricted solid-on-solid (RSOS) model [14] and body-centered solid-on-solid (BCSOS) model [15] have been proposed to study the kinetic roughening of the growth processes which belong to different universality classes. A competitive growth model consisting of two kinds of particles namely BD (with probability $1-p$) and RDSR (with probability p) was reported [16]. Two system-dependent crossover timescales t_c and τ were found to characterize the rough surface. In this model, scaling properties follow the RDSR model for $t \ll t_c$ while for $t \gg t_c$ BD scaling properties are dominant over the concerned regime. The nonlinear coupling (λ) is scaled with the abundance of the particles as $\lambda \sim p^{\gamma}$. The overall scaling was found to be

$$\begin{aligned} W_2(L,t) &\sim t^{\beta_{\mathrm{RDSR}}} && t \ll t_c \\ W_2(L,t) &\sim \lambda^{\beta_{\mathrm{BD}}} t^{\beta_{\mathrm{BD}}} && t_c \ll t \ll \tau \\ W_2(L,t) &\sim (C_1 + C_2 p^{3/2}) L^{\alpha} && t \gg \tau. \end{aligned} \tag{3}$$

The subscripts correspond to the respective models. C_1 and C_2 are constants. α is the same for both the models.

Several continuum models have also been prescribed to characterize the rough surfaces formed due to many natural growth processes [17]. The continuum linear growth model described by the Edward–Wilkinson (EW) equation [18] belongs to the same universality class as that of the discrete RDSR model. The values of α and β in (1+1) dimension for this universality class are given as $\alpha = 1/2$ and $\beta = 1/4$. The nonlinear Kardar–Parisi–Zhang (KPZ) equation [19] defines the universality class which includes the discrete growth models, such as the BD model, ED model, RSOS model and BCSOS model. In $(1+1)$ dimensions, the scaling exponents for this class are $\alpha = 1/2$ and $\beta = 1/3$ with the scaling identity

$$\alpha + \alpha/\beta = 2. \tag{4}$$

This scaling identity follows due to Galilean invariance of the interface [20]. However, nonlocality in the form of long-range interaction in the KPZ equation can modify the above identity [21–23].

Instead of a strong agreement between the theoretical and numerical predictions of α and β in the same universality class, the results do not match with several experimental findings. In (1+1) dimensions, experiments on immiscible fluid displacement show the roughness exponent

α lying between 0.73 and 0.89 [24–27]. Besides, experiment on growth of bacterial colonies [28] yields $\alpha = 0.81$. A possible explanation of the above-mentioned experimental results was proposed by Zhang [29]. He suggested a model with the noise amplitude having power-law distribution as $P(\eta(\vec{r}, t)) \sim \eta^{-(1+\mu)}$, where $\eta(\vec{r}, t)$ is the δ-correlated noise.

During recent decades, the growth of organic crystals on inorganic substrates draws great attention toward the application in electronic devices [30]. Thin-film growth of several organic crystals on different substrates [31–33] has been studied experimentally. One diffusion-limited-aggregation (DLA) type of discrete growth model [34] has been proposed to study the kinetic roughening of the growth of pentacene film on the SiO_2 substrate. The growth of organic crystals involves particles of large sizes, namely, the molecular formule of pentacene, copper phthalocyanin and 3,4,9,10-perylenetetracarboxylic dianhydride are $C_{22}H_{14}$, $C_{32}H_{16}N_8Cu$ and $C_{24}H_8O_6$, respectively.

Motivated by the above various growth mechanisms which involve small and extended particles with different types of relaxation rules, we have proposed a discrete growth model in (1+1) dimension. This model may involve particles of different sizes in a single growth process. In this model, the particle size plays a major role in the kinetic roughening of the surface. This model shows a morphological transition from the multifractal to unifractal regime beyond a system-dependent characteristic length scale [35]. The morphology of the surface depends on dominating particles in the growth process. The finite-size scaling relation is not of the universal type as defined in equation (2), not even satisfying equation (3). A new scaling relation is proposed to characterize the rough surface. The values of the scaling exponents α and β are not universal for this model. It has a finite-size dependence with a particular scaling form.

The paper is organized as follows. In section 2, we describe the model with the simulation parameters. In section 3, we propose the scaling law characterizing the rough surface. The effect of finite size on the scaling exponents is discussed in section 4. Porosity, a parameter that represents the bulk nature of the system, is introduced in a new scaling form in section 5. Finally, in section 6, the conclusions are drawn from the numerical results described in previous sections.

2. The model and its simulation

The model introduced here contains essentially the aggregation and diffusion mechanisms with a new idea of extended particles from a generalized point of view. The concept of these participating particles is introduced in such a way that the particles can be of various sizes for a single growth process. The diffusion mechanism considered here is the same for all types of particles. In spite of this, however, the final morphology of the surface is not the same when particles of different sizes are taking part in the growth process separately. A detailed description of the model is given below.

The substrate lattice is taken of size L with a periodic boundary condition. The participating particles in this model are considered as a different multiple matrix sequence in terms of the smallest unit of the substrate lattice. In this way, if the substrate lattice is considered as a $1 \times L$ matrix such that the smallest unit of this lattice is a 1×1 matrix , then the involving particles may be of sizes as 1×1 (), 1×2 (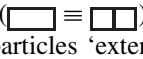), 2×1 () and so on. From this generalized point of view, we call the particles 'extended particles'. The units of 1×1 particles at the ends of each extended particles which are facing toward the substrate lattice will be called 'extreme cells'. In this sense, the particles 1×1, 2×1, 3×1, ... have only one extreme cell while the particles 1×2, 2×2, 1×3, ... have two extreme cells (see figure 1, extreme cells are shown as shaded boxes).

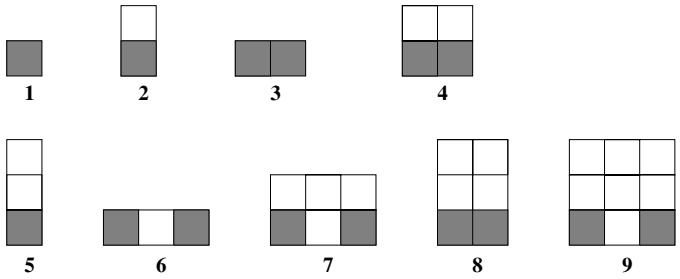

Figure 1. Different types of particles participating in the growth process. (1) is the 1×1 particle, (2) is the 2×1 particle, (3) is the 1×2 particle and so on. The shaded boxes of each particle are the extreme cells as defined in the text.

When these above-mentioned particles form the rough surface, a 'stable position' should be maintained throughout the surface for each of the involving particles. The stable position refers to a condition when at least one point from each of the extreme cells for each extended particle is in contact with the columns from the substrate lattice separately. In other words, the extended particles will attach with the substrate lattice if at least one corner from each extreme cell is shared with the corners of the columns from the substrate lattice. In this circumstance, the selection of the cell from the two extreme cells by the substrate lattice site is random. The overall aggregation and diffusion mechanism of the different types of particles is described as follows: one of the extreme cells from each of the extended particles is chosen randomly by a substrate site, then it (the extended particle) slides according to the lower height profile of the nearest-neighbor columns with a stable position. The process continues till the stable position is reached. Naturally, when the number of extreme cells is one, then the selection of this extreme cell by the substrate lattice site is completely deterministic.

It is obvious that the aggregation and diffusion mechanism of the 1×1 particles follows the RDSR mechanism [11]. The 2×1 particles also follow the RDSR mechanism except the height increment of the column at which it finally sticks is of two units rather than one, as with 1×1 particles. Similar rules are also valid for the relaxation mechanism of the particles of sizes 3×1, 4×1, ... But the case is quite different for the 1×2, 2×2, 1×3, ... particles. The mechanism of the diffusion of these particles is not of RDSR type. The growth rules are a straightforward generalization of the RDSR model for extended particles. It seems that the diffusion of each type of particle will cause different types of surface morphology. For clarification, we show in figures 2 and 3 schematically the aggregation and diffusion mechanism for the 1×2 and 1×3 particles, respectively. In both of these figures, one of the extreme cells (I and II) corresponding to the extended particles is chosen by a site (A) of the substrate lattice randomly.

With these rules, we have developed a model in $(1 + 1)$ dimensions with the participating particles having different sizes. The morphology of the surface should be determined by particles dominating the growth process. During the growth process, bulk defects are allowed to form. But the growth rules have been set in such a way that the voids formed in the system are closed, so that possible overhangs should be avoided. The lateral growth property breaks the up–down symmetry, resulting the presence of nonlinearity due to the local slope ($\nabla h(\vec{\mathbf{r}}, t)$) fluctuation in the continuum description of the model. It was previously reported [35] that the participation of the 2×1 particles in the growth process does not significantly change the morphology of the surface generated from the RDSR mechanism. Moreover, the 1×2 particles create voids in the system during surface growth, so KPZ type of growth characteristics may occur. Also the up–down symmetry is broken due to the involvement of the 1×2 particles

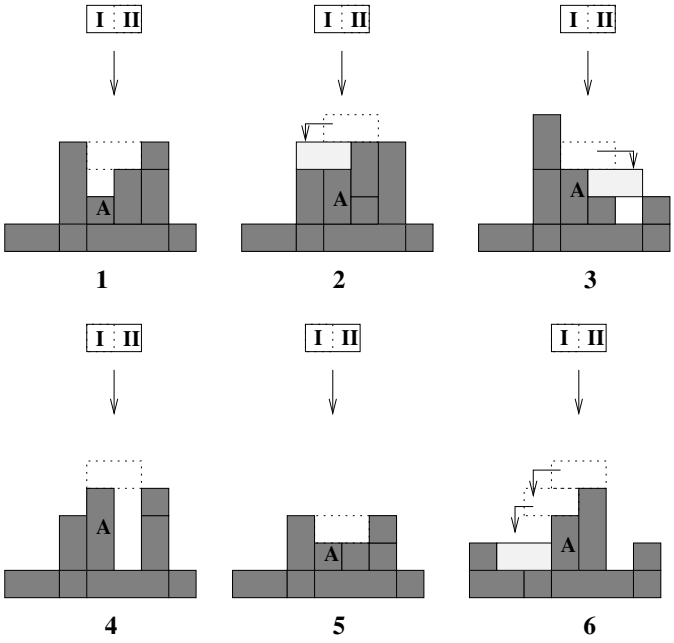

Figure 2. The aggregation and diffusion mechanism for 1×2 particles. Different possible cases are shown. Here one of the extreme cell (I) is chosen by a site (A) of the substrate lattice randomly. The case will be equivalent when the other extreme cell (II) is chosen by the site (A) of the substrate lattice.

in the growth process. So, the scaling properties of the kinetic roughening of the surface are expected to be modified by the nonlinearity introduced by 1×2 particles. For the above-mentioned reasons we have simulated the surface and analyzed its kinetic roughening for the surface formed due to the 1×2 particles only. The morphology of the surface formed due to the deposition of 1×2 particles for the system size $L = 200$ at time 2×10^2 is shown in figure 4 with four equal time zones. The increment of roughness of the surface with time is evident from the figure.

The model has been simulated in the lattices of lengths $L = 50 \times 2^n$ ($n = 0$ to $n = 6$). Deposition time is taken as $10^4 \leqslant t \leqslant 10^7$ depending upon the lattice size. The internal structure of the surface is characterized by 'intrinsic width' [36]. The probable origin of intrinsic width is the voids, overhangs and large local slopes. To minimize the effects from intrinsic width, we have incorporated the noise reduction technique [36]. The noise reduction parameter is the number of attempts per site for the actual aggregation process. In this model, the noise reduction parameter (m) was set fixed as $m = 10$. With this value of m the surface morphology shows a stable scaling behavior with repeated independent simulations. Uniformly distributed uncorrelated noise has been taken. Depending upon the system size, the results were averaged over 100 to 10 independent runs. Simulations were done on an IBM Server PC with two 64-bit quad-core POWER5+ processors.

3. Non-universal scaling of kinetic roughening of the surfaces

The kinetic roughening is characterized by the scaling exponents corresponding to the moments of height fluctuation defined in equation (1). The log–log plot of the second-order moment

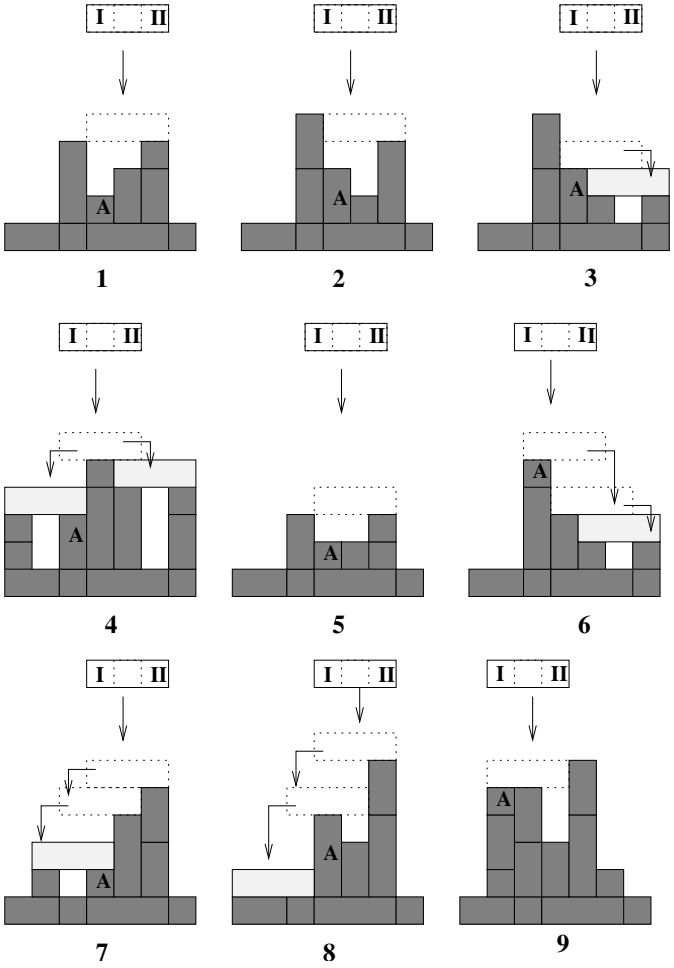

Figure 3. The deposition and relaxation mechanism for the 1×3 particles. Different possible cases are shown. A random lattice site (A) chooses one of the extreme cells (I) of the extended 1×3 particle randomly. The choice of another extreme cell (II) gives the statistically same type aggregation and diffusion mechanism.

of the height fluctuation for the values of lattice size $50 \leqslant L \leqslant 3200$ is shown in figure 5. It is clear from the figure that three distinct scaling regimes exist, which are separated by two timescales namely $t_{\times 1}$ and $t_{\times 2}$. The situation occurring around the crossover timescale $t_{\times 1}$ should not be confused with the situation occurring when the finite-size scaling is affected by the intrinsic width of the system because intrinsic width is a system size-independent effect [37]. The crossover between the intrinsic width affected regime with the unaffected regime is independent of the system size. But from figure 5 it is clear that the crossover $t_{\times 1}$ is system size dependent. The scaling form of the timescale $t_{\times 1}$ will be shown later.

To demonstrate the scaling behavior of the rough surface evolved from the present discrete model, the time evolution of the height fluctuation corresponding to a particular system size ($L = 400$) has been shown in figure 6. The nature of the plot in figure 6 is quite similar to that of the plot for the competitive growth model consisting of RDSR and BD [16]. But the situation is different here. Only one kind of particle is taking part in the growth process.

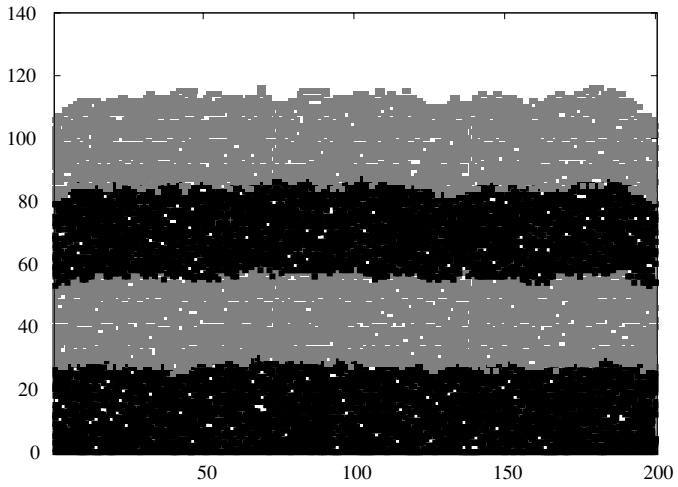

Figure 4. The rough surface formed due to the deposition of 1×2 particles. The total number of particles involved here has been isolated into four sets with different color shading showing the change in roughness.

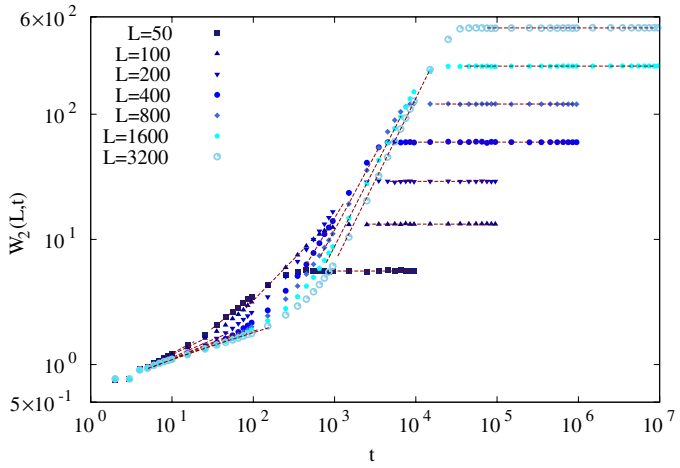

Figure 5. Log–log plot of $W_2(L, t)$, the second-order moment of the height fluctuation as defined from equation (1), versus t. The dotted lines are the power-law fitted according to equation (5) in three distinct regimes.

So, no other timescale can appear depending upon the abundances of the different kinds of particles participating in the growth process as in the discrete model described in [16]. Thus, the scaling behavior for the present model cannot be defined by equation (3). Guided by the nature of the scaling of a growth process [1], three power laws with different exponents have been fitted in three different scaling regimes as follows:

$$\begin{aligned} W(L,t) &\sim t^{\beta_1}, & t &\ll t_{\times 1}, \\ W(L,t) &\sim t^{\beta_2}, & t_{\times 1} &\ll t \ll t_{\times 2}, \\ W(L,t) &\sim L^{\alpha}, & t &\gg t_{\times 2}. \end{aligned} \tag{5}$$

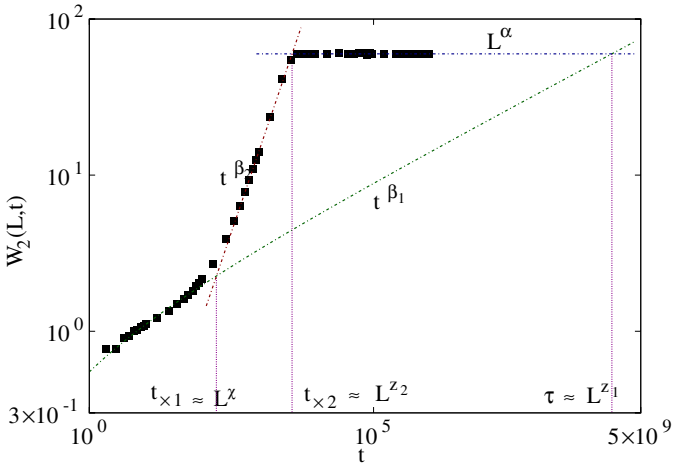

Figure 6. Representation of different scaling regimes of the second-order height fluctuation for a particular system size L=400 with the respective power-law fitting. This fit shows $\alpha = 0.698 \pm 0.002$, $\beta_1 = 0.22 \pm 0.02$ and $\beta_2 = 1.21 \pm 0.04$.

Also, in figure 5 the power-law fitting for different system sizes is shown by dotted lines. The scaling behavior shown in equation (5) indicates that, though the surface evolved with a definite mechanism, two different growth processes belonging to different universality classes are governing the overall kinetic roughening process. Such a scaling behavior of a growth model has not been noted previously in the literature. The system contains three characteristic timescales $t_{\times1}$, τ and $t_{\times2}$ (see figure 6). The timescale τ denotes the saturation time for a growth process belonging to a certain universality class with the growth exponents α and β_1. Another growth process belonging to a different universality class seems to occur beyond $t \sim t_{\times1}$ with the growth exponents α and β_2. From figure 6, we see that the two independent growth processes with saturation timescales τ and $t_{\times2}$ actually determine the crossover timescale $t_{\times1}$. So, the crossover timescale $t_{\times1}$ should depend on the timescales τ and $t_{\times2}$. The crucial timescale $t_{\times1}$ is the crossover between these two growth processes. The saturated rough surface is characterized by the latter growth process dominating beyond $t_{\times1}$. The timescales corresponding to the two distinguished growth processes should behave as

$$\tau \sim L^{z_1}$$
$$t_{\times2} \sim L^{z_2}. \tag{6}$$

Also from the nature of the height fluctuation (see figure 5) it can be argued that the crossover timescale $t_{\times1}$ can be scaled with the system size L as

$$t_{\times1} \sim L^{\chi}, \tag{7}$$

where $z_1 = \alpha/\beta_1$ and $z_2 = \alpha/\beta_2$ are the two dynamic exponents corresponding to the two growth processes occurring in two different time regimes, χ is a different scaling exponent. Since the crossover timescale $t_{\times1}$ is dependent on the other two independent timescales τ and $t_{\times1}$ so the scaling exponents χ depends naturally on the two independent exponents z_1 and z_2.

From the scaling behavior, we argue the simplest possibility that the kinetic roughening of the surface is occurring by the two growth processes in two different time regimes (namely, $t \ll t_{\times1}$ and $t \gg t_{\times1}$) independently. With this consideration, we propose that the overall morphology of the surface is governed by the scaling relation which can be represented as the

linear sum of two scaling functions corresponding to each of the growth process dominating in different regimes, leading to the saturated rough surface having a unique roughness exponent. So, mathematically, the proposed scaling relation can be represented as

$$W_2(L,t) \sim L^{\alpha}\left[f_1\left(\frac{t}{L^{z_1}}\right) + f_2\left(\frac{t}{L^{z_2}}\right)\right], \tag{8}$$

where the various scaling functions are defined by

$$\begin{aligned}
&f_1(u_1) \sim u_1^{\beta_1} && u_1 \ll \frac{1}{L^{z_1-\chi}}\\
&f_1(u_1) \sim \text{constant} && u_1 \gg \frac{1}{L^{z_1-\chi}}\\
&f_2(u_2) \sim \text{constant} && u_2 \ll \frac{1}{L^{z_2-\chi}}\\
&f_2(u_2) \sim u_2^{\beta_2} && \frac{1}{L^{z_2-\chi}} \ll u_2 \ll 1\\
&f_2(u_2) \sim \text{constant} && u_2 \gg 1.
\end{aligned} \tag{9}$$

To observe the appropriate scaling and the crossover, we proceed as follows. According to the scaling relation (8), in the time regime $t \ll t_{\times 1}$, i.e. for $t/L^{z_1} \ll 1/L^{z_1-\chi}$ the scaling functions f_1 and f_2 will be

$$\begin{aligned}
&f_1\left(\frac{t}{L^{z_1}}\right) \sim \left(\frac{t}{L^{z_1}}\right)^{\beta_1}\\
&f_2\left(\frac{t}{L^{z_2}}\right) \sim \text{constant}.
\end{aligned}$$

Thus from equation (8) the scaling relation becomes

$$W_2(L,t)/L^{\alpha} \sim \left(\frac{t}{L^{z_1}}\right)^{\beta_1} \qquad \text{when} \quad \frac{t}{L^{z_1}} \ll \frac{1}{L^{z_1-\chi}}. \tag{10}$$

For the time regime $t_{\times 1} \ll t \ll t_{\times 2}$ i.e., for $1/L^{z_2-\chi} \ll t/L^{z_2} \ll 1$ the scaling functions f_1 and f_2 will look like

$$\begin{aligned}
&f_1\left(\frac{t}{L^{z_1}}\right) \sim \text{constant}\\
&f_2\left(\frac{t}{L^{z_2}}\right) \sim \left(\frac{t}{L^{z_2}}\right)^{\beta_2}.
\end{aligned}$$

So according to equation (8) the scaling relation reduces to

$$W_2(L,t)/L^{\alpha} \sim \left(\frac{t}{L^{z_2}}\right)^{\beta_2} \qquad \text{when} \quad \frac{1}{L^{z_2-\chi}} \ll \frac{t}{L^{z_2}} \ll 1. \tag{11}$$

The time regime $t \gg t_{\times 2}$ i.e., when $t/L^{z_2} \gg 1$ the scaling functions f_1 and f_2 behave like

$$\begin{aligned}
&f_1\left(\frac{t}{L^{z_1}}\right) \sim \text{constant}\\
&f_2\left(\frac{t}{L^{z_2}}\right) \sim \text{constant}.
\end{aligned}$$

In this time regime, the scaling relation turns out to be

$$W_2(L,t)/L^{\alpha} \sim \text{constant when} \quad \frac{t}{L^{z_2}} \gg 1. \tag{12}$$

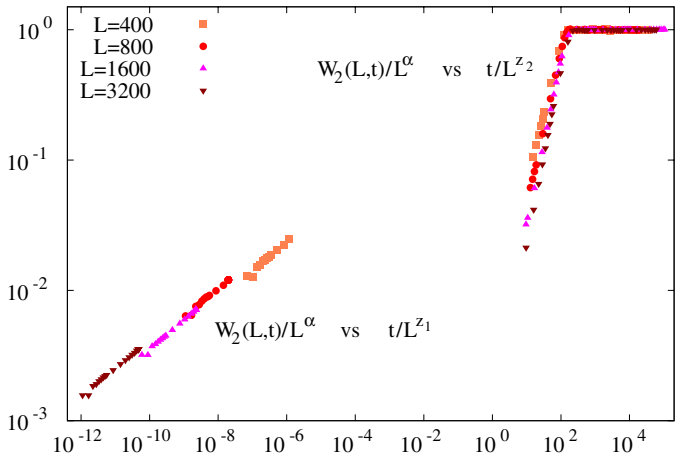

Figure 7. The scaling plot in the log–log scale shows that $W_2(L,t)/L^{\alpha}$ is plotted against t/L^{z_1} for $t \ll L^{z_1}$ and $W_2(L,t)/L^{\alpha}$ is plotted against t/L^{z_2} for $t \gg L^{z_1}$. As predicted from the scaling relation given by equation (8), two distinct scaling functions given by equation (9) are seen to exist prominently.

The above scaling relations in equations (10)–(12) satisfy the observation in equation (5). The complete data collapse in the log–log plot of $W_2(L,t)/L^{\alpha}$ in different time regimes as shown in figure 7 also confirms the above scaling relation.

Thus, for this discrete model, the kinetic roughening of the surface cannot be scaled with a unique scaling function having two independent scaling exponents. It thus deviates from the universal nature of the scaling of the kinetic roughening of the surfaces.

The visualization of the scaling relation defined in equation (8), with the scaling functions given in equation (9), is shown in figure 7 with the data collapse in two different time regimes $t \ll t_{\times 1}$ and $t \gg t_{\times 1}$. The scaling functions have been plotted for different sets of L, α, β_1 and β_2 values, because of the strong finite-size effect on α and weak finite-size effect on β_1 and β_2. Though the x-coordinate for each plot is different (one is t/L^{z_1} and the other is t/L^{z_2}), we plot in the same graph to show the existence of two distinguished scaling regimes $t \ll t_{\times 1}$ and $t \gg t_{\times 1}$. The large gap between the two scaling regimes, $t \ll t_{\times 1}$ and $t \gg t_{\times 1}$, is due to the large difference of two dynamic exponents z_1 and z_2. Also, the long crossover region around $t \sim t_{\times 1}$ is one of the reasons for such a large gap. The data collapse for scaling functions defined in equation (9) with the exponents defined in equation (5) for the respective time regimes defined in equations (6) and (7) confirms the scaling relation defined by equation (8).

The scaling behavior shown in figure 5 can be explained physically in the following way. In our model, the particles diffuse along the surface in search of a stable position. During the growth process, there is an interplay of diffusion with the finding of the stable position for each particle. Initially, since the total number of involved particles in the growth process is small, each particle is allowed to diffuse throughout the surface. So, within this time, diffusion of particles dominates over the process of finding the stable position. After the relaxation, when a 1×2 particle sticks to the substrate lattice, it implies that the constituent two 1×1 particles stick with the same height. Thus, from the 1×1 particle point of view the height–height fluctuation also decreases. For these two reasons, the overall height–height fluctuation of the surface during this time period will be very small, resulting in a small value of the dynamic exponent (β). However, with the increase of time, more and more particles take part in the growth process. Due to the relaxation rules there is a fair probability of getting a stable

position for each particle within the short-range sites. Effectively, the particles are restricted to the connected sites of the lattice site on which they were deposited. In other words, the particles are now localized almost stopping the long-range relaxation. Thus, an instability occurs due to the piling of particles on the upper terraces and restriction of the relaxation on the lower terraces. This increases the height–height fluctuation, resulting a large value of the dynamic exponent (β). This effect is quite similar to the Ehrlich–Schwoebel (ES) effect [39–43] which arises due to the presence of an ES barrier. This effect induces an instability by hindering step-edge atoms on upper terraces from going down to lower terraces in the MBE type of growth processes. A discrete solid-on-solid model [44] of epitaxial growth without the bulk defect was proposed, which takes into account the ES effect with the introduction of a parameter ($R_{\rm inc}$) called the incorporation radius as an ES barrier. Another reasonably realistic bulk defect-induced discrete model [45] of epitaxial growth in $(1+1)$ dimensions was presented in such a way so that the kinetic roughening is controlled by the interplay of the mound instability with the KPZ roughening. In this model, the diffusion of the particles was partially controlled by the parameter E, which actually selects the direction of diffusion with a probability $\exp(-E)$. In both of the above models, instability occurs due to the presence of a step-edge barrier; in the former case it is infinite while in the latter case it is finite. However, in our model, we do not place any step-edge barrier explicitly; the instability occurring here is completely self-organized.

The complicated scaling behavior of the rough surface evolving from the present discrete model is represented by a linear sum of two independent scaling functions corresponding to different growth processes. Now we point out the unusual behavior of the scaling function around $t \sim t_{\times 1}$. The crossover around $t_{\times 1}$ leads to a morphological 'phase transition' from one universality class to another. Such a morphological phase transition with a unique growth mechanism has not been observed previously for any discrete growth model. In this context, we may also mention that another morphological linear–nonlinear 'phase transition' is seen to occur around a critical probability of deposition of the 1×2 particles, beyond a characteristic length scale, for a competitive growth model involving particles of sizes 1×1, 2×1 and 1×2 [35]. Below we would like to study the variation of the roughness exponents with the system size L.

4. Finite-size effect on the roughness exponent

The earlier work by Krug and Meakin [38] has shown that for a nonlinear KPZ growth model the roughness exponents were affected by the finite-size dependence of the steady-state growth rate of the system. The demonstration of the finite-size effect on growth rate of evolution of the surface is shown first. The growth rate of the surface is defined as $V(L,t) = \frac{\mathrm{d}\langle h(t)\rangle}{\mathrm{d}t}$. According to the suggestion of Krug and Meakin [38], the steady-state growth rate is scaled with the system size L as

$$V(L, t \to \infty) = V(L \to \infty) - \Lambda L^{-\nu}. \tag{13}$$

The scaling behavior of velocity V in equation (13) is shown in figure 8. The fitting shows $\nu = 0.61 \pm 0.05$, with an asymptotic limit of the steady-state velocity is $V(L \to \infty) = 1.083 \pm 0.02$. It was predicted [38] that the roughness exponent for a large enough system for growth models belongs to the KPZ universality class, would be related to ν as

$$\alpha = 1 - \nu/2. \tag{14}$$

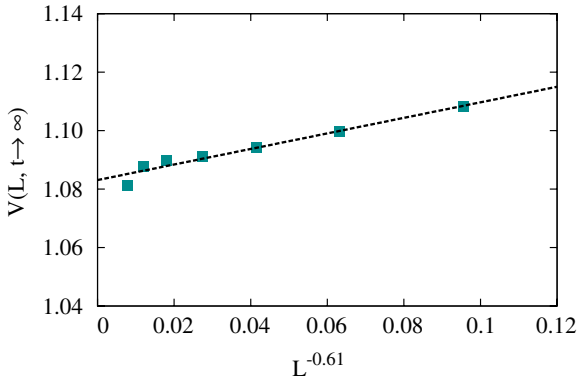

Figure 8. Fitting of steady-state velocity in the asymptotic limit versus $L^{-\nu}$ with $\nu = 0.61 \pm 0.05$.

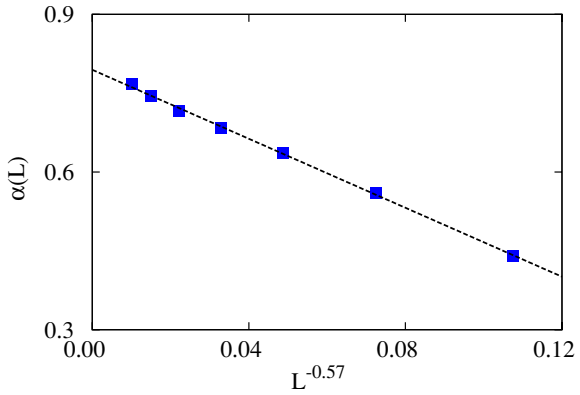

Figure 9. Finite-size dependence of the roughness exponent α. The fitting of α with $L^{-\delta}$ shows that $\delta = 0.57 \pm 0.03$.

The strong finite-size effect on α is also observed in the present model. The following scaling relation for the finite-size dependence on α was suggested [46] earlier:

$$\alpha(L) = \alpha(L \to \infty) + \Upsilon L^{-\delta}. \tag{15}$$

In figure 9, the α values are fitted according to the above scaling relation given by equation (15) with $\delta = 0.57 \pm 0.03$. For an asymptotically infinite system, the roughness exponent $\alpha(L \to \infty) = 0.794 \pm 0.005$ which is comparable with the prediction in equation (14). The relation between the exponents shown in equation (14) is based on the realization that the Family–Vicsek scaling relation (equation (2)) is satisfied. In the hydrodynamic limit, the present model satisfies the scaling relation given in equation (8) rather than in equation (2). So, it can be argued that the correction due to the finite-size dependence of the roughness exponent will be not like that of the model which follows KPZ type of growth. We have compared these two models because they both have inclination-dependent current due to the lateral growth property, which is the source of KPZ-like behavior in the growth process. Growth models with power-law distributed noise events $P(\eta(\vec{\mathbf{r}}, t)) \sim \eta^{-(1+\mu)}$ show such values of α [47, 48] with different values of μ. However, in our present model, the noise distribution is δ-correlated with uniform amplitude. Rare events are not occurring here. With the time evolution of the

system, a multifractal behavior is also seen to occur in the present model [35], similar in nature as that of the rare event dominated growth model [49].

The values of the two dynamic exponents β_1 and β_2 remain steady for a large system size. The values of these two dynamic exponents are found to be $\beta_1 = 0.22 \pm 0.03$ and $\beta_2 = 1.22 \pm 0.01$ for large enough systems. Such a large value of the dynamic exponent β_2 has still not been observed in the literature. Due to strong finite-size dependence of α and weak finite-size effect on the values of β_1 and β_2, the crossover timescale $t_{\times 1}$ is dependent on the system size L with an exponent χ as given in equation (7). Moreover, $\alpha + z_1 \neq 2$ and $\alpha + z_2 \neq 2$; this immediately points out the breakdown of the Galilean invariance of the system. It is to be noted that the value of the dynamic exponent β_1 is very close to that of the EW model with $\beta_1 = \frac{1}{4}$. Above the system-dependent timescale $t \sim t_{\times 1}$ the dynamic exponent β_2 has a very high value. The transition of the dynamic exponent from a low to a higher value can be visualized by looking critically to the individual configuration of the surface and the bulk. As per the aggregation and diffusion rules, it appears that initially the surface moves compactly without having voids and that is why the dynamic exponent (β_1) in that region is close to that of the RDSR model. At later times, voids are incorporated into the system and an ES-like instability is found to occur. This self-organized ES effect triggers the rapid roughening of the surface. The dynamic exponent (β_2) becomes high in that region. The experimental observation of rapid roughening involving extended particles in the growth of organic thin film (diindenoperylene) was reported previously [50].

5. Bulk properties and its scaling

To obtain a deep insight into the internal structure of the interface, the bulk properties of the system are of great interest. The diffusion mechanism for the present growth model is unique by its definition. Closed voids created due to such a diffusion mechanism made the system porous in its own way. So, the bulk property will be different from the other porous systems, created from different kinds of aggregation and diffusion mechanisms. The bulk properties of a system can be quantified with the definition of porosity. Since the number of closed voids can be determined accurately, we define, porosity P for this particular system in a similar way as defined in [51]:

$$P = N_v/N_t, \tag{16}$$

where N_v = number of voids and N_t = number of voids + number of particles deposited. A deposition process where the number of particles is conserved, is characterized by the particle flux J. As shown by Krug [52], the deposit density ρ can be related to the growth velocity v as

$$\rho = J/v. \tag{17}$$

According to equation (17), the deposit density, which actually characterized by the quantity porosity, will be scaled with the system size as that of the velocity with the modification due to the particle flux dependence on the system size in the asymptotic limit. To see the asymptotic limit of the porous structure of the system at saturation with system size, we propose a scaling relation of the porosity as

$$P(L, t \to \infty) = P(L \to \infty) + \Gamma L^{-\eta}. \tag{18}$$

The above-proposed scaling relation is new in the present literature.

From the physical point of view, porosity can be defined as the reverse of the deposit density. That is

$$P = 1 - \rho. \tag{19}$$

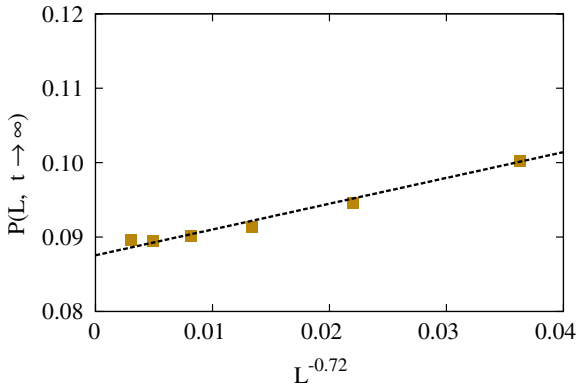

Figure 10. Plot of porosity in the asymptotic limit with $L^{-\eta}$ with the exponent $\eta = 0.72 \pm 0.02$.

From equation (17) for uniform flux J

$$1 - P = J/v, \qquad P \sim v - 1. \tag{20}$$

Figure 10 shows the behavior of the porosity at the asymptotic limit with different system sizes. It shows that asymptotic value of the porosity $P(L \to \infty)$ as 0.087 ± 0.005 and the coefficient $\Gamma = 0.34 \pm 0.013$. The prediction from equation (20) is well in agreement with the results shown in figures 8 and 10.

6. Conclusion

The kinetic roughening of a surface created due to a nonlinear discrete growth model is studied here. Several features, not previously observed corresponding to kinetic roughening, are observed in the present model in (1+1) dimensions. To summarize, we mention the following points systematically. The finite-size scaling of the rough surface shows a different type scaling nature. Two distinct timescales, corresponding to the height fluctuation, emerge in the system in (1+1) dimensions. They separate three scaling regimes with different scaling exponents as well as scaling functions. To characterize this kinetic roughening, a new scaling relation is proposed, which is represented as the linear sum of two scaling functions valid for two distinct scaling regimes. The existence of two scaling regimes with small and large values of the dynamic exponent β is well explained with the occurrence of a self-organized ES like instability (caused due to the localization of the extended particles) which triggers the rapid roughening of the surface. Due to the finite-size effect on the growth rate, the scaling exponents are also affected by the finite size of the system. The finite-size effect on the roughness exponent is scaled with a scaling relation. The scaling exponent for this scaling relation compares well with the prediction made by Krug and Meakin. The bulk nature of the system for different sizes is shown through a new scaling relation.

Acknowledgments

One of the authors (PKM) would like to thank the University Grant Commission (UGC), New Delhi, India for financial support to carry out this work. We are grateful to DST-FIST, New Delhi, India for providing us the necessary help. We are indebted to the anonymous referees for critical suggestions and comments.

References

[1] Barabási A-L and Stanley H E *Fractal Concepts in Surface Growth* (Cambridge: Cambridge University Press)
[2] Meakin P 1993 *Phys. Rep.* **235** 189
[3] Healy T H and Zhang Y-C 1995 *Phys. Rep.* **254** 215
[4] Alava M, Dubé M and Rost M 2004 *Adv. Phys.* **53** 83
[5] Amaral L A N, Barabási A L, Buldyrev S V, Havlin S and Stanley H E 1994 *Phys. Rev. Lett.* **72** 641
[6] Kumar P B S and Jana D 1996 *Physica* A **224** 199 (arXiv:9509047)
[7] Albano E V, Salvarezza R C, Vázquez L and Arvia A J 1999 *Phys. Rev.* B **59** 7354
[8] Kardar M 2000 *Physica* A **281** 295
[9] Ben-jacob E, Schochet O, Tenenbaum A, Cohen I, Czirók A and Vicsek T 1994 *Fractals* **2** 15
[10] Family F and Vicsek T 1985 *J. Phys. A: Math. Gen.* **18** L75
[11] Family F 1990 *J. Phys. A: Math. Gen.* **19** L441
[12] Vold M J 1959 *J. Colloid Interface Sci.* **14** 168
Vold M J 1959 *J. Phys. Chem.* **63** 68
[13] Parisi G and Zhang Y-C 1984 *Phys. Rev. Lett.* **53** 1791
[14] Kim J M and Kosterlitz J M 1989 *Phys. Rev. Lett.* **62** 2289
[15] Chin C-S and den Nijs M 1999 *Phys. Rev.* E **59** 2633
[16] Chame A and Aarão Reis F D A 2002 *Phys. Rev.* E **66** 051104
[17] Marsili M, Maritan A, Toigo F and Banavar J R 1996 *Rev. Mod. Phys.* **68** 963
[18] Edwards S F and Wilkinson D R 1982 *Proc. R. Soc.* A **381** 17
[19] Kardar M, Parisi G and Zhang Y-C 1986 *Phys. Rev. Lett.* **56** 889
[20] Medina E, Hwa T, Kardar M and Zhang Y-C 1989 *Phys. Rev.* A **39** 3053
[21] Mukherji S and Bhattarcharjee S M 1997 *Phys. Rev. Lett.* **79** 2502
[22] Jung Y, Kim I M and Kim J M 1998 *Phys. Rev.* E **58** 5467
[23] Chattopadhyay A K 1999 *Phys. Rev.* E **60** 293
[24] Rubio M A, Dougherty A and Gollub J P 1990 *Phys. Rev. Lett.* **65** 1389
[25] Rubio M A, Edwards C A, Dougherty A and Gollub J P 1989 *Phys. Rev. Lett.* **63** 1685
[26] Horváth V K, Family F and Vicsek T 1990 *Phys. Rev. Lett.* **65** 1388
[27] Horváth V K, Family F and Vicsek T 1991 *J. Phys. A: Math. Gen.* **24** L25
[28] Vicsek T, Cserö M and Horváth V K 1990 *Physica* A **167** 315
[29] Zhang Y-C 1990 *J. Phys.* **51** 2129
[30] Schreiber F 2004 *Phys. Status Solidi* b **201** 1037
[31] Kunstmann T, Schlarb A, Fendrich M, Wagner Th and Möller R 2005 *Phys. Rev.* B **71** 121403
[32] Fendrich M, Wagner Th, Stöhr M and Möller R 2006 *Phys. Rev.* B **73** 115433
[33] Krause B, Schreiber F and Dosch H 2004 *Europhys. Lett.* **65** 372
[34] Zorba S, Shapir Y and Gao Y 2006 *Phys. Rev.* B **74** 245410
[35] Mandal P K and Jana D 2008 *Phys. Rev.* E **77** 061604
[36] Wolf D E and Kertész J 1987 *J. Phys. A: Math. Gen.* **20** L257
[37] Kertész J and Wolf D E 1988 *J. Phys. A: Math. Gen.* **21** 747
[38] Krug J and Meakin P 1990 *J. Phys. A: Math. Gen.* **23** L987
[39] Ehrlich G and Hudda E G 1966 *J. Chem. Phys.* **44** 1039
[40] Schwoebel R L and Shipsey E J 1966 *J. Appl. Phys.* **37** 3682
[41] Schwoebel R L 1969 *J. Appl. Phys.* **40** 614
[42] Krug J 1997 *Adv. Phys.* **46** 139
[43] Politi P, Grenet G, Marty A, Ponchet A and Villain J 2000 *Phys. Rep.* **324** 271
[44] Beihl M and Schinzer S 1998 *Europhys. Lett.* **41** 443
[45] Schimschak M and Krug J 1995 *Phys. Rev.* B **52** 8550
[46] Aarão Reis F D A 2004 *Phys. Rev.* E **69** 021610
[47] Buldyrev S V, Havlin S, Kertész J, Stanley H E and Vicsek T 1991 *Phys. Rev.* A **43** 7113
[48] Lam C-H and Sander L M 1993 *Phys. Rev.* E **48** 979
[49] Barabási A-L, Bourbonnais R, Jensen M, Kertész J, Vicsek T and Zhang Y-C 1992 *Phys. Rev.* A **45** R6951
[50] Dürr A C, Schreiber F, Ritley K A, Kruppa V, Dosch H and Struth B 2003 *Phys. Rev. Lett.* **90** 016104
[51] Silveira F A and Aarão Reis F D A 2007 *Phys. Rev.* E **75** 061608
[52] Krug J 1989 *J. Phys. A: Math. Gen.* **22** L769